Finite element modelling on Micro-machining of graphene reinforced aluminum matrix composites

Hao Yu (ABC2642910499@163.com)
Civil Aviation University of China
Zhenpeng He
Jinbo Li
Baichun Li
Jia Xin
Lianzheng Yao
Fangchao Yan

Research Article

Keywords: Finite element mode, Graphene, Metal matrix composites, Micro-machining, Cutting mechanism

Posted Date: May 16th, 2022

DOI: https://doi.org/10.21203/rs.3.rs-1631698/v1

Finite element modelling on Micro-machining of graphene reinforced aluminum matrix composites

Hao Yu[1] · Zhenpeng He [1] · Jinbo Li[2] · Baichun Li[1] · Jia Xin[1] · Lianzheng Yao[1] · Fangchao Yan[3]

1 College of Aeronautical Engineering, Civil Aviation University of China, Tianjin, 300300, China

2 School of Mechanical Engineering, Shenyang University of Technology, Shenyang, 110870, China

3 Tianjin Bu Er Technology Co., Ltd, Tianjin, 300300, China

Baichun Li

bc_li@cauc.edu.cn

Abstract

Graphene reinforced metal matrix composites have received a lot of attention from academia and industry due to their excellent mechanical properties. In this paper, the machinability of graphene reinforced aluminum metal matrix composites (Gr/Al MMCs) during micro-machining is investigated by finite element method. A three-dimensional modeling program based on the Python language is developed independently, this program can generate graphene with random distribution of orientation and position. A three-dimensional two-phase finite element model considering the cutting edge radius is established to simulate the micro-machining process of Gr/Al MMCs. Embedded element method is used in the model to more efficiently simulate the interaction behavior between graphene and aluminum matrix during micro-machining. The accuracy of the model is verified by indirect experiments. Stress distribution, tool-graphene interaction, chip formation, cutting force and specific cutting energy during micro-machining are investigated with different uncut chip thickness. The simulation results show that graphene inhibits stress propagation, resulting in the formation of a stress field with irregular contours within the matrix. Continuous serrated chips are generated during the cutting process. The addition of graphene increases the magnitude and fluctuation of cutting forces.

Keywords Finite element mode · Graphene · Metal matrix composites · Micro-machining · Cutting mechanism

1 Introduction

Due to their properties such as high specific strength, fatigue resistance, wear resistance and low density, aluminum matrix composites have been widely used in aerospace, automotive industry and

defense in recent years [1].

The traditional reinforcements for aluminum matrix composites are mainly silicon carbide particles, carbon fibers and alumina particles [2,3]. With the discovery of graphene, it has become a more attractive nano-reinforced material for improving the properties of metals with its excellent mechanical properties. Graphene is a two-dimensional material composed of carbon atoms in a single hexagonal honeycomb structure [4]. In graphene, three of the four valence electrons in each carbon atom form a strong and stable structure by sp^2 orbital hybridization [5]. The strong chemical bonds between carbon atoms give graphene excellent structural rigidity and mechanical properties. Graphene has a Young's modulus of 1.1 TPA and a tensile strength of 130 GPa [6]. The room temperature thermal conductivity of graphene is about 5000 w / (m · K) [7]. In addition, graphene has a large specific surface area (2630 m^2/g), which enhances the interfacial interactions and results in better mechanical properties of graphene-reinforced metal matrix composites. Bishta et al. [8] prepared Gr / Al MMCs by spark plasma sintering. The results showed that the yield strength and tensile strength of the composites were increased by 84.5% and 54.8%, respectively, when the graphene nanoplatelet content was 1 wt%. Lou et al. [9] obtained graphene nanoplatelet-reinforced aluminum composites by hot extrusion process. The tensile strength of GNP/Al composites was improved by 11.2%, while the increase in plasticity was not significant. In general, graphene is used as a reinforcement for aluminum matrix composites, which significantly improved the properties of aluminum.

Aluminum matrix composites are used in aviation, electronics and other high precision or micro parts. Micro-machining is considered as one of the most widely used micro-manufacturing methods. Understanding the micro-machining process of aluminum matrix composites can help to improve the machining process. Unlike macro-machining processes, the size effect of micro-machining processes is more pronounced as the ratio of uncut chip thickness to cutting edge radius decreases. Na et al. [10] studied the effects of different graphene contents on chip morphology, milling force and machined surface morphology of Gr / Al MMCs during micro-milling. The experimental results showed that the milling force is maximum when graphene mass fraction is 1%. With the increase of graphene content, the chip morphology of the composites gradually changes from crack morphology to continuous morphology. Liu et al. [11] investigated the effect of tool angle on 45 vol.% SiCp / 2024Al micro-machining. It was shown that a proper tool rake angle can effectively suppress tool wear, reduce SiCp shedding and improve the machined surface quality. Teng et al. [12] investigated the micro-machinability of nanoparticle reinforced magnesium matrix composites. The cutting forces, surface morphology and size effects during micro-milling were analyzed. Compared with the experimental method, the finite element method can clearly show the stresses and strains in the matrix and reinforcement during machining processing. Gao et al. [13] developed a two-dimensional finite element cutting model of metal matrix nanocomposites considering the random distribution of graphene nanosheets in the matrix. The effect of different parameters on the cutting force was investigated by this model. It was shown that the cutting depth has the greatest effect on the cutting force. Teng et al. [14] established a two-dimensional finite element micro-machining model of nano SiC / Mg metal matrix composites considering the tool cutting radius. The tool-particle interaction, stress distribution, cutting forces and chip formation processes were investigated at different uncut chip thicknesses. The simulation results show that the SiC nanoparticles limit the stress propagation and remain intact during the machining process. When the uncut chip thickness is greater than 1 μm, continuous serrated chips are formed. Liu et al. [15]

investigated the effects of cutting speed and tool-particle interaction on the surface formation mechanism of micro-machined SiCp / Al composites. The results showed that the surface roughness of SiCp/Al composites decreased with increasing cutting speed, and high feed per tooth exacerbated the fracture of SiCp. There is very limited research on the micro-machining process of Gr / Al MMCs. The stress and strain of the aluminum matrix and graphene reinforcement during micro-machining of Gr / Al MMCs are not well understood. It is necessary to investigate the effect of graphene on the aluminum matrix to improve the machining techniques of Gr / Al MMCs.

In this paper, Gr / Al MMCs three-dimensional modeling program based on python is developed. A finite element model is developed to study the micro-machining process of Gr / Al MMCs considering the cutting edge radius. Unlike previous studies, the random distribution and deformation of graphene in three-dimensional space are considered in this model. The validity of the model is verified by indirect experiments. The distribution of stress and strain, tool-graphene interactions, chip formation, cutting forces and specific cutting energy of Gr / Al MMCs during micro-machining are investigated.

2 Finite element modelling procedures

2.1 Geometric modeling of micro-machining

The mechanical properties of Gr / Al MMCs are greatly changed due to the incorporation of graphene reinforcement. The macroscopic mechanical properties of the Gr / Al MMCs are isotropic. However, the effects of the position and orientation of graphene on aluminum matrix cannot be ignored when the uncut chip thickness is in the micron range. Therefore, it is necessary to develop a microscopic model of Gr / Al MMCs that is close to the actual situation. The number of graphene in the representative volume element (RVE) should be calculate. The mass fraction of Gr / Al MMCs can be converted into volume fraction by the following [16]:

$$V = \frac{\rho_C}{\rho_G} w \tag{1}$$

$$\rho_C = \rho_G V + \rho_M V_M \tag{2}$$

where V is the volume fraction of the graphene; w is the weight fraction of the graphene; ρ_C, ρ_G and ρ_M are the densities of the Gr / Al MMCs, graphene and aluminum matrix, respectively; V_M is the volume fraction of aluminum matrix. Bring Eq.2 into Eq.1 and rearrange to get the following:

$$V = \frac{w}{w + \left(\rho_G / \rho_M\right)\left(1 - w\right)} \tag{3}$$

The amount of graphene contained in the matrix can be calculated as follows:

$$N = \left(\frac{V_{RVE}}{V_G}\right) V \tag{4}$$

where V_{RVE} is the volume of RVE, V_G is the volume of graphene. The size of RVE is 20 μm × 4 μm × 5 μm. The mass fraction of Gr / Al MMCs is set to 0.5%. Assume that the graphene edge length is 1 μm and the thickness is 20 nm. Due to the high aspect ratio of the graphene reinforcement, the graphene is equivalent to a variable shell. Different from particle reinforced aluminum matrix composites such as SiC and Al_2O_3, graphene has completely different mechanical properties in different directions [17]. Therefore, it is necessary to consider the orientation of graphene in the aluminum matrix. Based on the Python language, the random generation of graphene in position and orientation is achieved by a random distribution algorithm (RDA). Due to the high graphene content, this RDA cannot currently ensure that all graphene will not intersect when the required number of graphene is generated. It is necessary to adjust the position of a small amount of cross-graphene after all graphene is generated. Fig. 1 shows the flow chart of the graphene formation process.

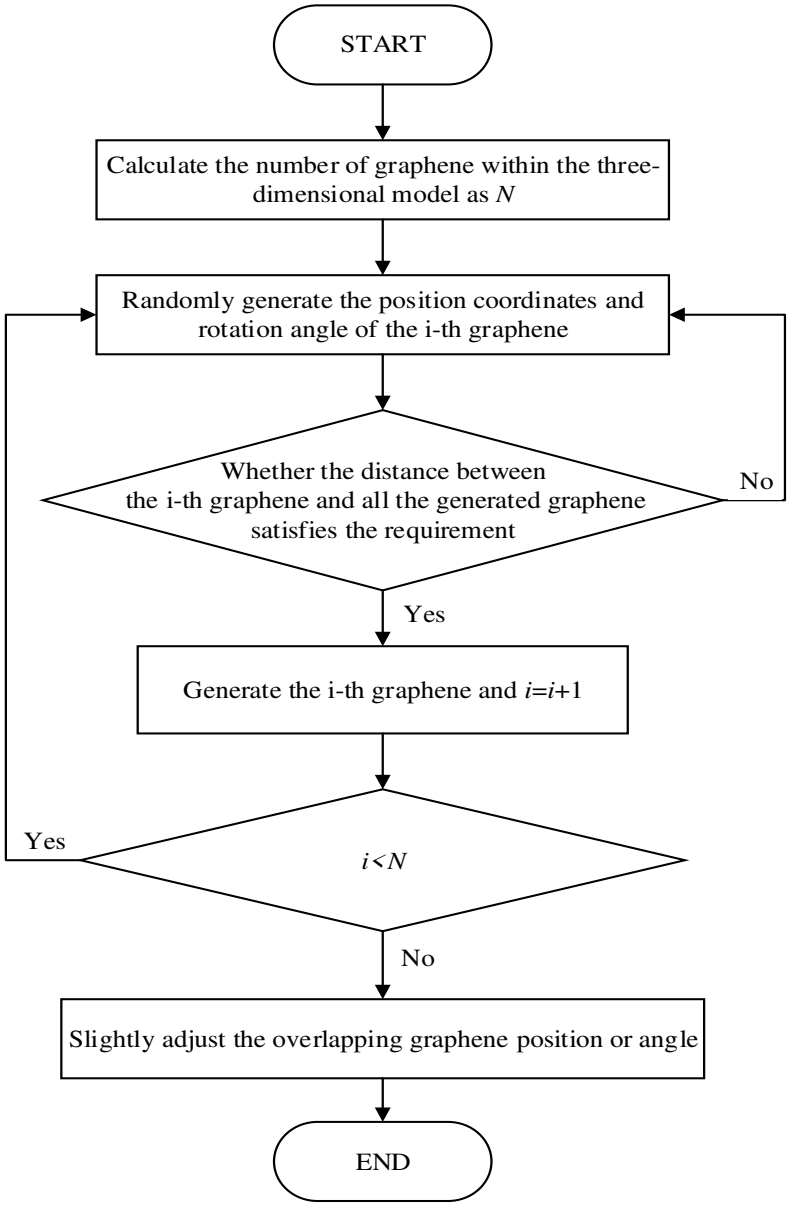

Fig. 1 Flow chart of graphene generation process

Conventional methods of cohesive zone elements and tied node to simulate composite interface behavior require that the mesh at the reinforcement-matrix interface must be identical. Due to the large number of randomly distributed graphene sheets in the model, the conventional method generates a large number of elements, which may lead to high computational cost and non-convergence [18]. The embedded element method is used to specify that an element or group of elements is embedded in host elements. The degrees of freedom of the embedding nodes are restricted to the matrix element nodes close to the nodes, and the appropriate weight coefficients are determined based on the geometric position. Therefore, graphene and aluminum matrix can be meshed separately without strictly meeting the consistency of interface mesh [19]. Liu et al. [20] developed the RVE finite element model of discontinuous fiber reinforced composites using the embedded element method. The results showed that the embedded element method can predict the mechanical properties of the composites well. Therefore, the mechanical transfer between graphene and aluminum matrix is accomplished by the embedded element method in this paper. The modeling process of Gr / Al MMCs RVE is shown in Fig. 2.

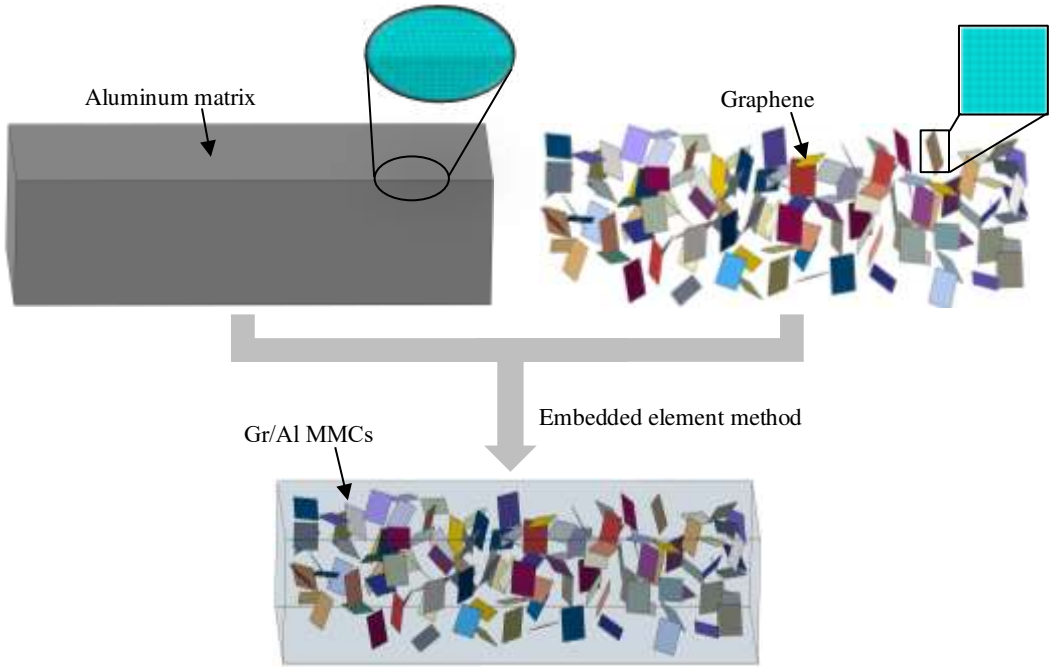

Fig. 2 Illustration of the modeling process of Gr / Al MMCs RVE

In this paper, a three-dimensional two-phase finite element cutting model of Gr / Al MMCs is established using ABAQUS software. The mesh size of aluminum matrix and graphene reinforcement is defined as 0.1 μm. The element types of the aluminum matrix and graphene reinforcement are C3D8R and S4R, respectively. The tool is reduced to a rigid body because the tool is much harder than the Gr / Al MMCs. The micro-machining model of the Gr / Al MMCs is shown in Fig. 3. Although the embedded element method can greatly reduce the number of meshes, the computational process is still complicated. An appropriate mass scale is used to improve the computational efficiency. The machining parameters are listed in Table 1. The intense deformation of the material during the cutting process leads to a significant increase in the material temperature. Therefore, adiabatic heating effects are considered in this paper.

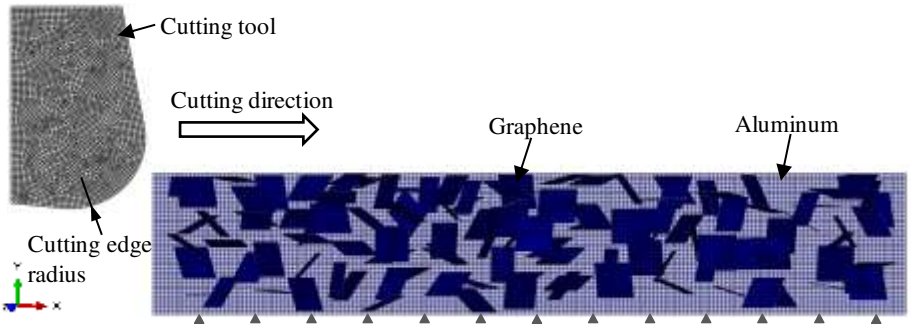

Fig. 3 Illustration of the micro-machining model of Gr / Al MMCs

Table 1 Machining parameters in FE model

Parameters	Values
Cutting speed, Vc (m/min)	62.83
Uncut chip thickness, t (μm)	0.25, 0.5, 0.75, 1, 1.25,1.5
Tool rake angle,α (Degree)	10
Tool clearance angle,β (Degree)	6
Cutting edge radius, (μm)	2

2.2 Materials constitutive model

The Johnson-Cook constitutive model can well describe the stress and strain behavior of materials at large strains, high strain rates and high temperatures. The Johnson-Cook constitutive model is simple and convenient, and it has been widely used in machining simulation. The Johnson-Cook constitutive model is shown as:

$$\sigma_f = \left[A + B(\bar{\varepsilon}^{pl})^n\right]\left[1 + C\ln\left(\frac{\dot{\bar{\varepsilon}}^{pl}}{\dot{\bar{\varepsilon}}_0}\right)\right]\left[1 - \left(\frac{T - T_r}{T_m - T_r}\right)^m\right] \tag{5}$$

where σ_f is the flow stress, $\bar{\varepsilon}^{pl}$ is the plastic strain, $\dot{\bar{\varepsilon}}^{pl}$ is the plastic strain rate, $\dot{\bar{\varepsilon}}_0$ is the reference strain rate, T is the workpiece temperature, T_r and T_m are the ambient temperature and material melting point. Coefficient A is the yield strength, B is the hardening modulus, C is strain rate sensitivity coefficient, n is the hardening coefficient, m is the thermal softening coefficient. The model parameters of aluminium in Johnson-Cook constitutive model are listed in Table 2.

Table 2 Parameters of material properties for aluminum [21]

Parameters	Values
Density (g/cm^3)	2.7
Youg's modulus (MPa)	70000
Poisson's ratio	0.27
A (MPa)	148
B (MPa)	361
C	0.001
m	0.859
n	0.183
T_m (K)	1220
T_r (K)	298

The Johnson-Cook dynamic failure model is used to define the failure criterion of matrix during machining process. The matrix fails when the damage parameter D exceeds 1. The damage parameter D is defined as:

$$D = \sum \left(\frac{\Delta \bar{\varepsilon}^{pl}}{\bar{\varepsilon}_f^{pl}} \right) \tag{6}$$

where $\Delta \bar{\varepsilon}^{pl}$ is an increment of equivalent plastic strain, $\bar{\varepsilon}_f^{pl}$ is the failure strain at the current time step for the stress state, strain rate and temperature. Failure strain $\bar{\varepsilon}_f^{pl}$ can be expressed as:

$$\bar{\varepsilon}_f^{pl} = \left[d_1 + d_2 \exp(d_3 \frac{p}{q}) \right] \left[1 + d_4 \ln \left(\frac{\dot{\bar{\varepsilon}}^{pl}}{\dot{\varepsilon}_0} \right) \right] \left[1 + d_5 \left(\frac{T - T_r}{T_m - T_r} \right) \right] \tag{7}$$

where d_1 - d_5 (list in Table 2) are fracture parameters measured below the transition temperature , p is the pressure stress, q is the von Mises stress. The parameters of Johnson-Cook dynamic failure model are listed in Table 3.

Table 3 Parameters of Johnson-Cook failure model for aluminum [21]

Parameters	Values
d_1	0.071
d_2	1.248
d_3	-1.142
d_4	0.147
d_5	0.1

There is a linear relationship between stress and strain in graphene, therefore it is considered as a linear elastic material [22]. Graphene fractures without a distinct plastic phase and therefore a brittle fracture model is used to define the graphene fracture criterion [23]. The material parameters of graphene are shown in Table 4.

Table 4 Material properties for Graphene [24,25,26]

Parameters	Values
Density (g/cm^3)	2.267
Youg's modulus (GPa)	1000
Poisson's ratio	0.186
Tensile strength (GPa)	130

2.3 Contact definitions and boundary conditions

The surface-to-surface contact (Explicit) model is used between the tool surface, graphene reinforcement and aluminum matrix. Sliding friction and sticking friction are the two main types of Coulomb friction. The Coulomb friction model is used to calculate the frictional stress on the contact surface as follows:

$$\begin{cases} \tau_f = \mu \sigma_n \quad \text{when} \quad \mu \sigma_n < \tau \quad (\text{sliding friction}) \\ \tau_f = \tau \quad \text{when} \quad \mu \sigma_n \geq \tau \quad (\text{sticking friction}) \end{cases} \tag{8}$$

where τ_f is the frictional stress on the interface, σ_n is normal stress distribution along the tool, τ is the ultimate shear stress at the interface, μ is the coefficient of friction. The friction coefficient μ is defined as 0.6 in this study [10]. The bottom surface of the model is fixed. Due to the extrusion of the side material, the movement of the model sides in the axial direction of the tool is restricted.

3 Results and discussion

In this section, the micro-machining process of Gr / Al MMCs will be analyzed from the aspects of stress distribution of aluminum matrix and graphene reinforcement, chip formation process and cutting force. Due to the small size of graphene, there are a large number of graphene sheets even in a small volume. Therefore, the increased values of cutting forces between Gr / Al MMCs and pure aluminum are used to indirectly verify the validity of the finite element cutting model. Na [10] carried out micro-milling experiments on 0.5 wt% Gr / Al MMCs using end mill with a cutting edge radius of 2 μm. At uncut chip thicknesses of 0.25, 0.5, 0.75, 1, 1.25, and 1.5 μm, compared with that of pure aluminum, the cutting force of Gr / Al MMCs increased by 7.5%, 12.4%, 11.2%, 4% and 12.5%, respectively. The simulation results show that the cutting forces increases by 6.2%, 4.3%, 8.4%, 2.9%, and 3.6%, respectively, under the same machining conditions. This suggests that the three-dimensional Gr / Al MMCs finite element model can simulate the strengthening effect of graphene on the aluminum matrix. The large errors between some simulated and experimental results may be due to the inhomogeneous distribution of graphene in the model. The increase in the simulated cutting force is slightly lower than the experimental value. This may be due to the fact that graphene inhibits the coarsening and growth of the aluminum matrix grains, and the smaller grains improve the mechanical properties of the aluminum matrix, making the actual cutting force larger than the simulated value.

3.1 Von Mises stress distribution of aluminum matrix

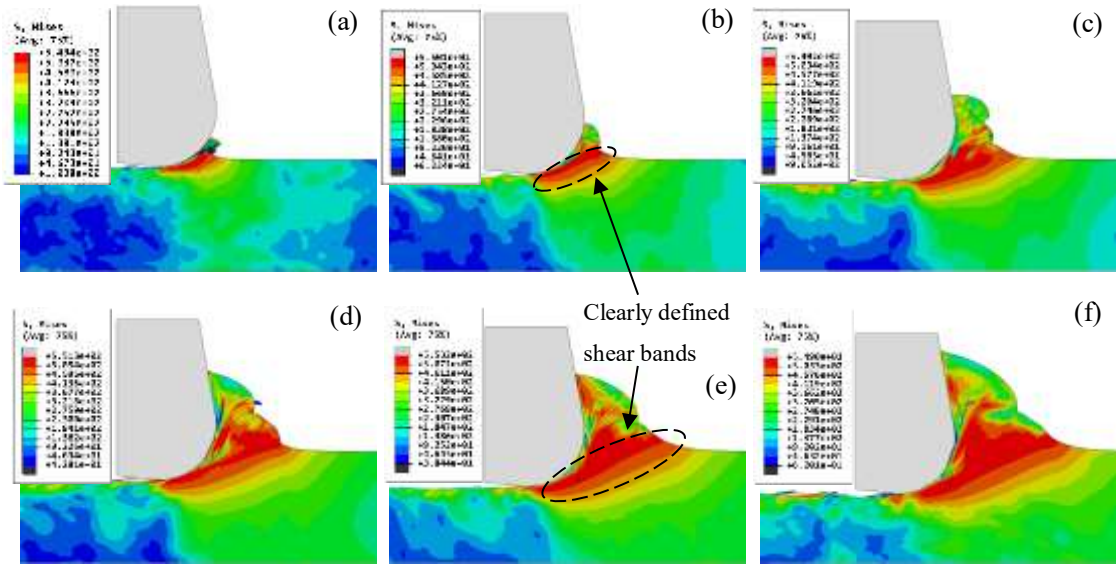

Fig. 4 von Mises stress distribution of aluminum at uncut chip thickness of (**a**) 0.25 μm, (**b**) 0.5 μm, (**c**) 0.75 μm, (**d**) 1.0 μm, (**e**) 1.25 μm, (**f**) 1.5 μm

As shown in Fig. 4, clear defined shear bands are formed in aluminum at different uncut chip thickness. Fig. 5 shows that the stress distribution of Gr / Al MMCs is different from that of aluminum. The addition of graphene greatly changes the stress distribution in the aluminum matrix.

It can be found that the added graphene acts as a barrier, limiting the propagation of stress (as show in Fig. 5b-f). In the process of micro-machining, von Mises stress field of irregular contour is formed in the aluminum matrix, as shown in Fig. 5c. By observing the von Mises stress distribution in Fig. 5d, the deformed stress contour can be found near graphene. A low stress region is formed near the graphene reinforcement. This is because the high-strength graphene undertakes great stress in the cutting process and reduces the stress of the matrix material near the graphene reinforcement. When a continuous chip is formed, the maximum stress in the aluminum matrix decreases slightly as the uncut chip thickness increases and then remains basically at about 550 MPa. The position of the aluminum matrix shear band is roughly the same as that of the aluminum shear band, which is located in the first deformation zone during the cutting process.

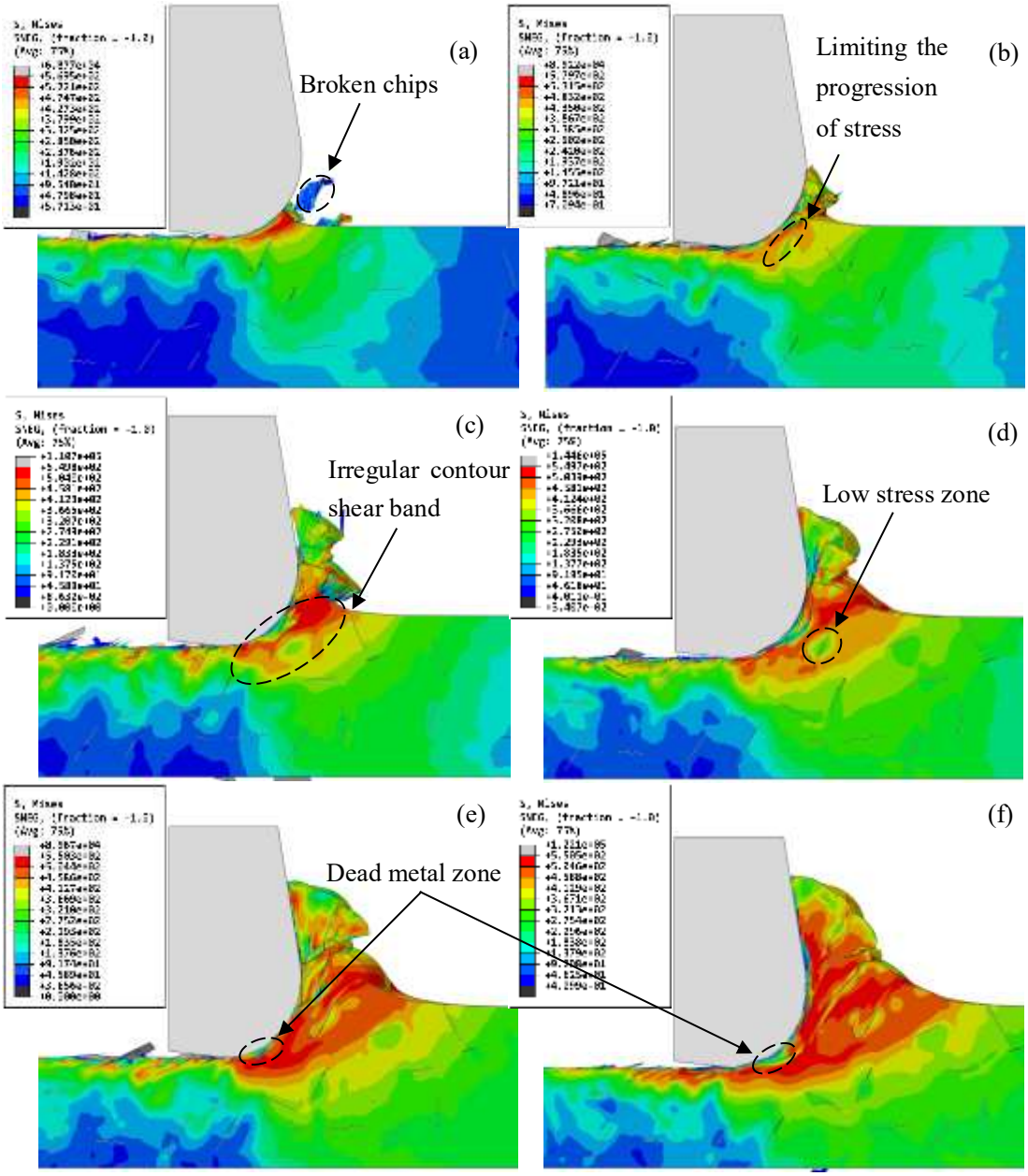

Fig. 5 Von Mises stress distribution of Gr / Al MMCs at uncut chip thickness of (**a**) 0.25 μm, (**b**) 0.5 μm, (**c**) 0.75 μm, (**d**) 1.0 μm, (**e**) 1.25 μm, (**f**) 1.5 μm

In the process of Gr / Al MMCs micro-machining simulation, a unique machining phenomenon

different from the macro-machining process is observed: when the uncut chip thickness is greater than 0.5 μm, a low stress zone appeared at the tool tip, which is similar to the stagnation state in the material flow. This region is referred to as the metal dead zone. The location of the metal dead zone is approximately the same as the location of the strain band generation in Fig. 10. This suggests that the metal dead zone may be related to the chip formation process.

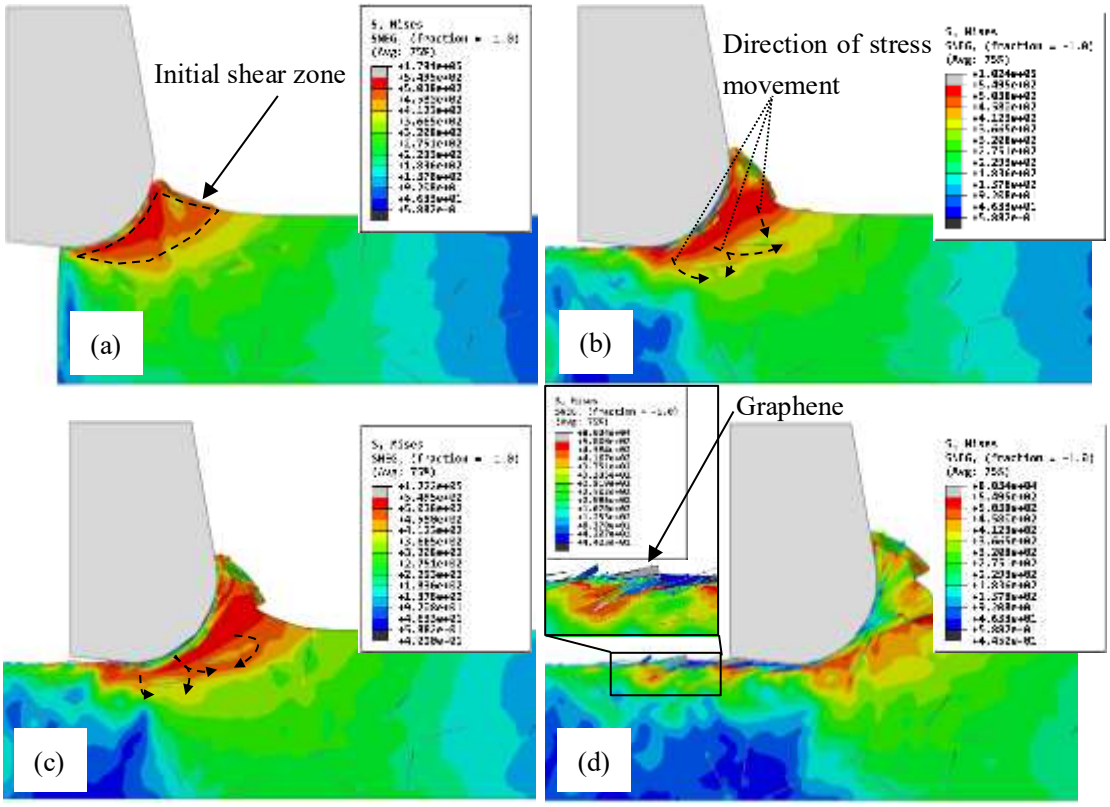

Fig. 6 von Mises stress distribution of aluminum matrix at uncut chip thickness of 0.75μm (**a**) 2.4 μs, (**b**) 4.4 μs, (**c**) 5.2 μs, (**d**) 8.0 μs

Fig. 6 illustrates the von Mises stress distribution of aluminum matrix during micro-machining at uncut chip thickness of 0.75 μm. As shown in Fig. 6a, the initial shear zone forms in the aluminum matrix when the tool makes initial contact with the Gr / Al MMCs and moves forward as the tool advances. In Fig. 6b-c, it can be observed that the stress tends to bypass the graphene when the shear band encounters the graphene, resulting in an irregular shear band profile. This phenomenon shows that graphene inhibits the propagation of stress in aluminum matrix, which is consistent with the phenomenon observed in the polymer/GNP cutting model developed by Fu [25]. Unlike the micro-machining process for aluminum, large residual stress can be observed on the machined surface, as shown in Fig. 6d. This phenomenon can be attributed to the friction between the graphene reinforcement and the tool during the machining process. The graphene pulls the aluminum matrix to produce plastic strain, which results in high residual stresses on the machined surface along the tool advancement direction. From the above, it can be seen that there are two modes of action of graphene on the aluminum matrix. The stress distribution of the aluminum matrix near the graphene is different in the two modes. The bond between graphene and matrix is always well maintained in either mode.

3.2 Interaction between tool and graphene reinforcement

Fig. 7 shows the von Mises stress distribution of graphene during micro-machining of Gr / Al MMCs at uncut chip thickness of 1 μm. As shown in Fig. 7a, graphene sheets start to be subjected to low stress in the initial stage due to the effect of deformation of the aluminum matrix. Fig. 7b illustrates that the deformation of graphene sheets in the aluminum matrix gradually increases as the tool advances, and the graphene sheets subject increased stress. The region where graphene sheets subject high stress is mainly located in the chips and shallow machined surfaces, which is basically the same as the high strain region of the aluminum matrix in Fig. 10b. The von Mises stress of graphene reinforcement is significantly higher than that of aluminum matrix. This phenomenon indicates that the load transferred from aluminum matrix during cutting is mainly subject by graphene. The graphene sheets below the cutting edge of the tool subject the most stress due to the extrusion and friction between the cutting edge and graphene. A small portion of the graphene sheets are broken at the edges. During the cutting process, most of the graphene sheets can keep their structures intact, which proves that graphene can withstand high von-Mises stresses during micro-machining.

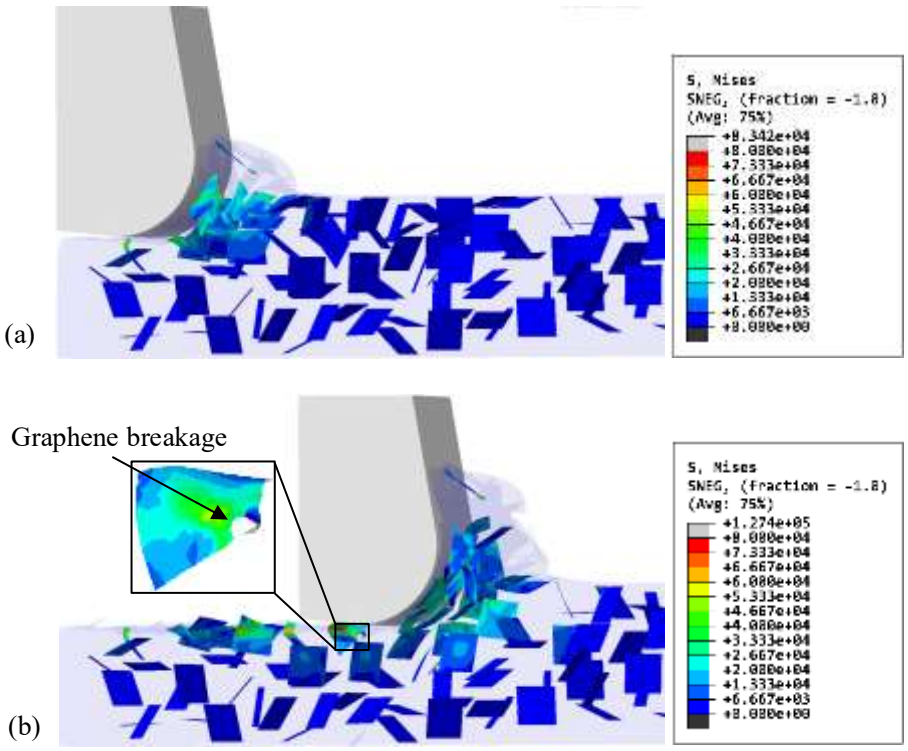

Fig. 7 von Mises stress distribution of graphene during micro-machining of Gr / Al MMC

Analyzing the interaction between tool and reinforcement is better to understand the machinability of composites and to predict tool wear. Fig. 8 shows the evolution of stress and deformation of graphene located below the cutting edge with the advancement of the tool. As shown in Fig. 8a, graphene starts to contact with the tool and deforms. Fig. 8a-c illustrates that graphene bends along the advancing direction of the tool due to the extrusion of the tool on the graphene. As shown in Fig. 8c, there is a clear stress concentration zone at the bend of graphene. At this time, the von Mises stress on graphene is the largest. It can be observed from Fig. 8d that the bending deformation of graphene partially recovers after the tool passes.

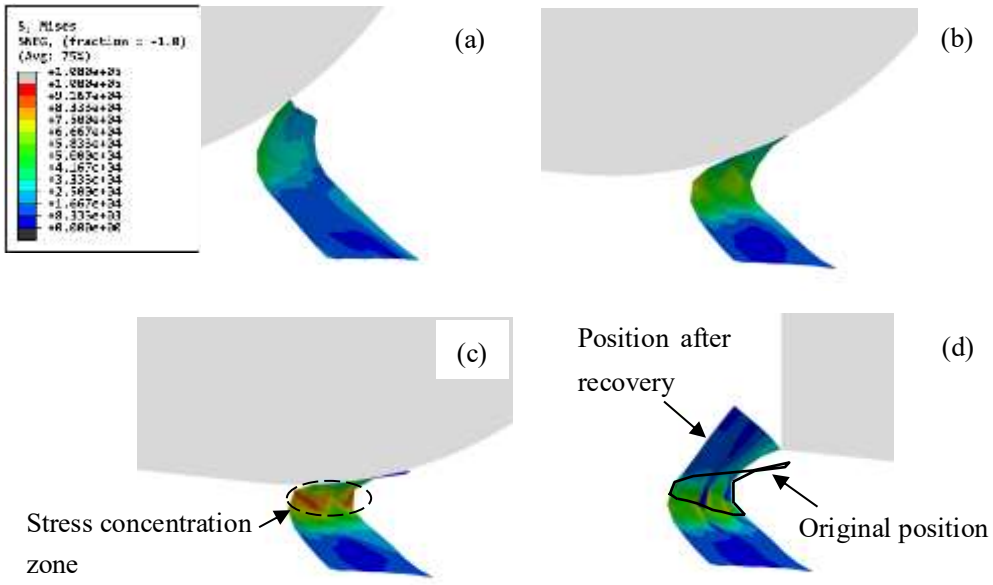

Fig. 8 Change of graphene located below the cutting edge with tool advancement

In precision machining process, the quality of the machined surface is an important factor affecting the performance of the workpiece. The simulated microscopic morphology of the machined surface of Gr / Al MMCs can be observed from Fig. 9. Because graphene is easily deformed, it does not produce holes and scratches on the machined surface as silicon carbide particles do during the machining process. Good surface quality can be obtained on the machined surface of Gr / Al MMCs. One part of the graphene is exposed and the other part is embedded in the matrix. Graphene sheets embedded in the machined surface reduce the contact area between the tool and the matrix and can act as a lubricant during the cutting process. Na et al. [10] found that graphene can prevent the generation and expansion of microcracks and micro holes during machining.

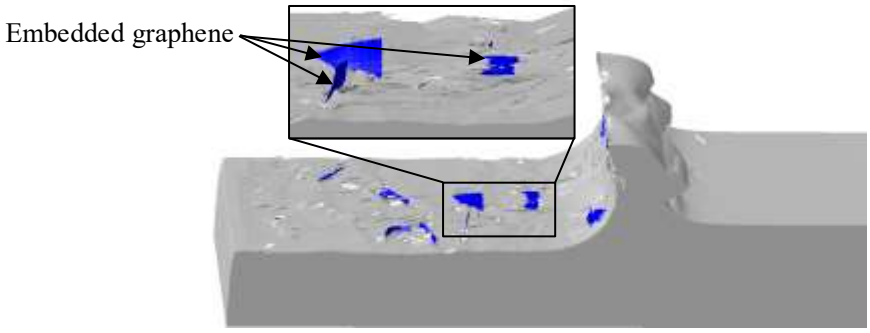

Fig. 9 Simulated micro morphology of Gr / Al MMCs machined surfaces

3.3 Chip formation process analysis

Fig. 5a also illustrates that the aluminum matrix is extruded by the tool and accumulates in front of the cutting edge, forming a small amount of broken chips. This is the reason when the uncut chip thickness decreases to a certain value, only part of the cutting edge of the tool is participating in the micro-machining process. The nominal rake angle of the tool has no effect on the cutting process and a negative rake angle occurs in the actual cutting process. At this time, the interaction between the tool and the aluminum matrix is mainly caused by the friction generated by the ploughing. The shear force required for the plastic deformation of the chip is insufficient, and most of the aluminum matrix is pressed into the workpiece, and a small portion is crushed to produce a broken chip. Fig.

5b-f illustrates that the ploughing effect decreases as the uncut chip thickness increases. The aluminum in front of the tool tip begins to damage and separate from aluminum matrix. The separated aluminum matrix moves along the rake face of the tool. This means that chips begin to form. During this process, graphene sheets above the cutting path move with the surrounding aluminum matrix and enter the formed chip as the tool advances.

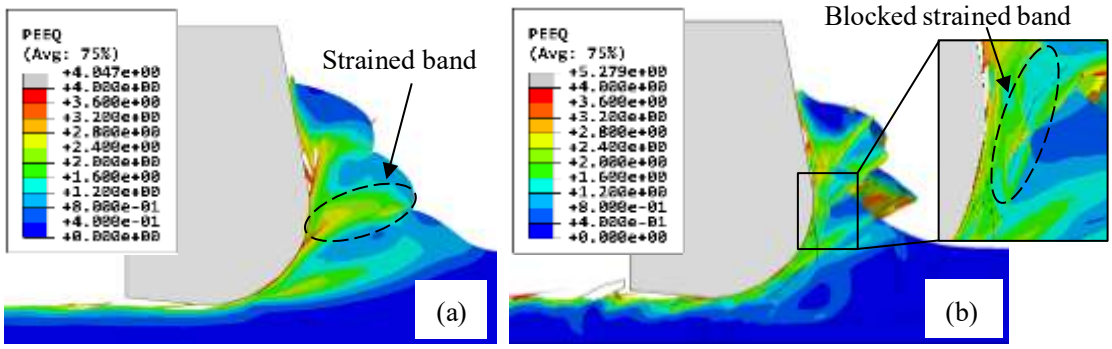

Fig. 10 Distribution of equivalent plastic strain comparison between (**a**) aluminum; (**b**) Gr / Al MMCs

It can be observed from Fig. 10a that with the advance of the tool, a slender strain zone is formed near the tool tip and extends to the upper surface of the aluminum. Regular strain band is formed in the chip. The process is repeated to form a continuous chip with regular shape, as shown in Fig. 11a. The position and orientation of graphene are important factors determining the propagation of stress and strain. Therefore, the chip shape in the micro-machining of Gr / Al MMCs is related to the position and orientation of graphene. As shown in Fig. 10b, the high strength graphene sheets in the chip restrict the expansion of the strain band. Irregular strain bands are generated in the chip. As shown in Fig. 11b, cracks can be observed on the chip surface and a serrated chip is formed. This is due to the random distribution of graphene within the matrix, and this inhomogeneous microstructure leads to excessive local strain during deforming process, which leads to matrix tearing. Gao [13] established a two-dimensional micro-machining model of graphene reinforced metal matrix nanocomposites with a cutting depth equal to the average size of graphene. With this model, it can be observed that discontinuous serrated chips are formed during the micro-machining process. This phenomenon is different from the continuous serrated chips observed in Fig. 10b, which may be due to the fact that the chips may not break in the cutting depth direction when the cutting depth is larger than the size of graphene. The phenomena observed by the model in this paper are generally consistent with the chip shape described in the paper of Na [10].

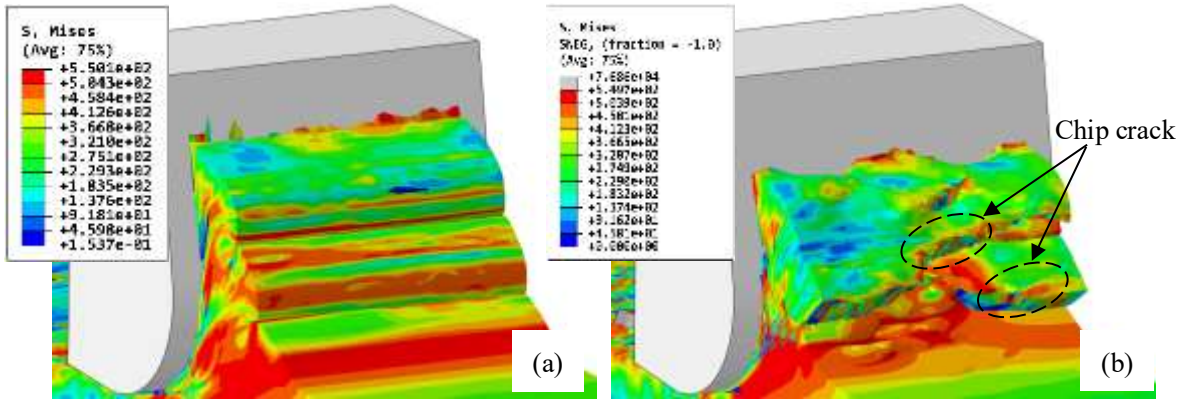

Fig. 11 Chip morphology comparison between (**a**) aluminum; (**b**) Gr / Al MMCs

3.4 Cutting force

Fig. 12 shows the simulated cutting forces and specific cutting energy for Gr / Al MMCs with uncut chip thicknesses of 0.25, 0.5, 0.75, 1, 1.25 and 1.5 μm, respectively. As shown in Fig. 4, the cutting force increases with the increasing of the uncut chip thickness, while the specific cutting energy decreases nonlinearly. This is due to the size effect of the micro-machining process. The fluctuation of the cutting force increases significantly with the increasing of the uncut chip thickness.

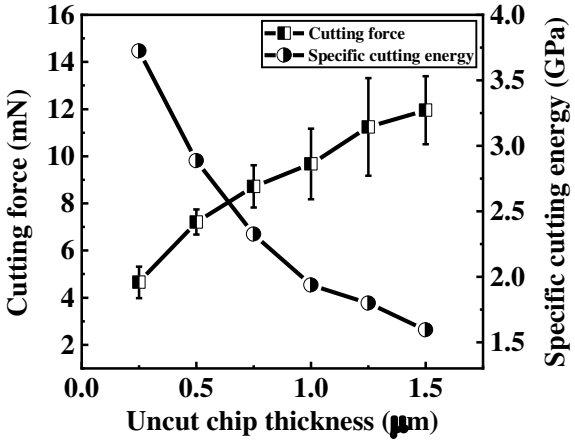

Fig. 12 Simulated cutting force and specific cutting energy of Gr / Al MMCs at different uncut chip thickness

Fig. 13 shows the simulated cutting forces change over time for machining aluminum and Gr/Al MMCs with an uncut chip thickness of 1 μm. The two cutting forces increase rapidly in the initial stage. Then they gradually transition to stable stage and fluctuates within a certain range. In contrast, the cutting force fluctuation of micro-machined Gr / Al MMCs is more pronounced than that of aluminum. The reason may be that the graphene reinforcement effect leads to non-uniform material properties. During the cutting of aluminum, periodic strain bands are generated due to the piling effect in front of the tool, resulting in periodic fluctuations of cutting force. This phenomenon is not evident in the cutting process of Gr / Al MMCs. This is due to the addition of graphene that disrupts the periodic formation of strain bands.

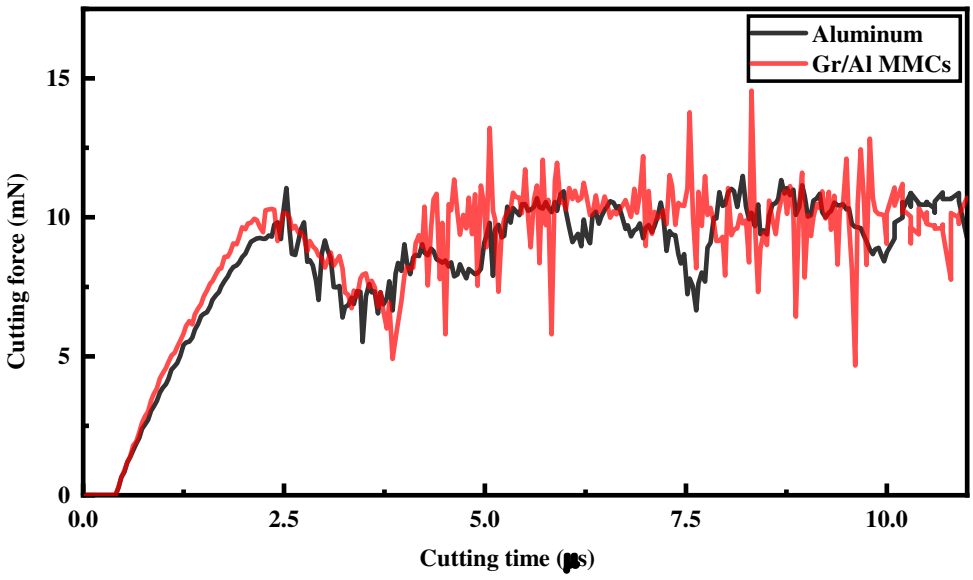

Fig. 13 Simulated cutting force of aluminum and Gr / Al MMCs at uncut chip thickness of 1μm

4 Conclusions

In the micro-machining process of Gr / Al MMCs, the stress and strain distribution, interaction of tool-graphene, chip formation and cutting force are studied. The main conclusions of this paper can be summarized as follows:

1. A Python-based structural modeling program is developed to generate graphene randomly distributed in position and orientation in three-dimensional space. A three-dimensional microstructure model of Gr/Al MMCs with a similar structure to the actual one is developed. In addition, the deformation of graphene during micromachining is considered in the model.
2. Graphene acts as a barrier, limiting the extension of stress and strain in the aluminum matrix, leading to the formation of irregular von Mises stress distributions and continuous serrated chips.
3. The location of graphene subjected to high von Mises during micro-machining is essentially the same as the large strain region of the matrix. The von Mises stress of graphene is much higher than that of matrix. Most graphene sheets can remain intact during cutting process. The maximum von Mises stress on graphene is located at the contact between the lower cutting edge and the machined surface due to tool extrusion and friction on the graphene.
4. The addition of graphene reduces the tool- matrix contact but increases the fluctuation of cutting force during cutting. The accuracy of the finite element model is indirectly verified by comparing with the increased value of experimental cutting force.

Funding The research presented in this document was supported by the Scientific Research Project of Tianjin Municipal Education Commission (2020KJ015), the Research Fund for the Natural Science Project of Tianjin Education Commission(2018KJ240) and the Tianjin excellent special agent project(20YDTPJC01720)

Author Contributions Zhenpeng He and Baichun Li contributed to the conception and design of this study. Hao Yu, Zhenpeng He and Jinbo Li were involved in the finite element modeling and simulation results analysis. Baichun Li, Fangchao Yan developed a Python-based modeling program. Jia Xin and Lianzheng Yao was involved in the data collection and made constructive suggestions. The first draft of the manuscript was written by Hao Yu and all authors commented on previous versions of the manuscript. All authors read and approved the final manuscript.

Availability of data and material The data and data sources relevant to this study are disclosed in the manuscript.

Declarations

Competing interests The authors have no relevant financial or non-financial interests to disclose.

Ethics approval All the authors of the manuscript agreed to participate.

Consent to participate All authors voluntarily participated in the work of this paper

Consent for publication All the authors of the manuscript agreed to publish this paper in

References

1. Bastwros M, Kim GY, Zhu C, Zhang K, Wang S, Tang X, Wang X (2014) Effect of ball milling on graphene reinforced Al6061 composite fabricated by semi-solid sintering. Composites Part B Engineering, 60(apr.), 111-118.
2. Ayar MS, George PM, Patel RR (2021) Advanced research progresses in aluminium metal matrix composites: An overview. PROCEEDINGS OF THE 14TH ASIA-PACIFIC PHYSICS CONFERENCE.
3. Mohammed S, Chen DL (2019) A review on carbon nanotube reinforced aluminum matrix composites. Advanced Engineering Materials, 22(4).
4. Rafiee MA, Rafiee J, Yu ZZ, Koratkar N (2009) Buckling resistant graphene nanocomposites. Applied Physics Letters, 95(22), 8535.
5. Lozovik YE, Merkulova SP, Sokolik AA, Morozov SV, Novoselov KS, Geim AK (2008) Collective electron phenomena and electron transport in graphene Scientific Session of the Physical Sciences Division of the Russian Academy of Sciences (27 February 2008). Physics-Uspekhi, 51(7), 727.
6. Lee C, Wei X, Kysar JW, Hone J (2008) Measurement of the elastic properties and intrinsic strength of monolayer graphene. science, 321(5887), 385-388.
7. Berger C, Song Z, Li T, Li X, Ogbazghi AY, Feng R, et al. (2004) Ultrathin epitaxial graphite: 2D electron gas properties and a route toward graphene-based nanoelectronics. j.phys.chem, 108(52), 19912-19916.
8. Bisht A, Srivastava M, Kumar RM, Lahiri I, Lahiri D (2017) Strengthening mechanism in graphene nanoplatelets reinforced aluminum composite fabricated through spark plasma sintering. Materials Science and Engineering: A, 695, 20-28.
9. Lou S, Liu Y, Qu C, Guo G, Ran L, Zhang P, Su C (2021) Influence of a Hot Extrusion with Rectangular-Section on Mechanical Properties and Microstructure of 0.5 wt% Graphene Nanoplate-Reinforced Aluminum Composites. Advanced Engineering Materials, 23(4), 2001127.
10. Na HB, Xu LH, Han GC, Liu SK, Lu LH (2019) Machinability research on the micro-milling for graphene nano-flakes reinforced aluminum alloy. Metals, 9(10), 1102.
11. Liu HZ, Wang SJ, Zong WJ (2019) Tool rake angle selection in micro-machining of 45 vol.% SiCp/2024Al based on its brittle-plastic properties. Journal of Manufacturing Processes, 37(JAN.), 556-562.
12. Teng X, D Huo, Wong E, Meenashisundaram G, Gupta M (2016) Micro-machinability of nanoparticle-reinforced Mg-based MMCs: an experimental investigation. The International Journal of Advanced Manufacturing Technology, 87(5), 2165-2178.
13. Gao Chongyang, Jia Jiguang. (2017). Factor analysis of key parameters on cutting force in micromachining of graphene-reinforced magnesium matrix nanocomposites based on FE simulation. International Journal of Advanced Manufacturing Technology.
14. Teng X, Huo D, Chen W, Wong E, Zheng L, Shyha I (2018) Finite element modelling on cutting mechanism of nano Mg/SiC metal matrix composites considering cutting edge radius. Journal of Manufacturing Processes, 32(APR.), 116-126.
15. Liu J, Cheng K, Ding H, Chen S, Zhao L (2018) Simulation study of the influence of cutting

speed and tool–particle interaction location on surface formation mechanism in micromachining SiCp/Al composites. Proceedings of the Institution of Mechanical Engineers, Part C: Journal of Mechanical Engineering Science, 232(11), 2044-2056.

16. Rafiee MA, Rafiee J, Wang Z, Song H, Yu ZZ, Koratkar N (2009) Enhanced mechanical properties of nanocomposites at low graphene content. ACS nano, 3(12), 3884-3890.
17. Yang XS, Zhou L, Liu KY, Liu ZY, Ma ZY (2021) Finite element prediction of the thermal conductivity of GNP/Al composites. Acta Metallurgica Sinica (English Letters).
18. Goudarzi M, Simone A (2019) Discrete inclusion models for reinforced composites: comparative performance analysis and modeling challenges. Computer Methods in Applied Mechanics and Engineering, 355(Oct.1), 535-557.
19. Dalbosco M, Carniel TA, Fancello EA, Holzapfel GA (2021) Multiscale numerical analyses of arterial tissue with embedded elements in the finite strain regime. Computer Methods in Applied Mechanics and Engineering, 381.
20. Liu H, D Zeng, Li Y, Jiang L (2016) Development of RVE-embedded solid elements model for predicting effective elastic constants of discontinuous fiber reinforced composites. Mechanics of Materials, 93(FEB.), 109-123.
21. Fathipour M, Hamedi M, Yousefi R (2013) Numerical and experimental analysis of machining of Al (20 vol% SiC) composite by the use of ABAQUS software. Materialwissenschaft und Werkstofftechnik, 44(1), 14-20.
22. Paci JT, Belytschko T, Schatz GC (2007) Computational studies of the structure, behavior upon heating, and mechanical properties of graphite oxide. J.phys.chem.c, 111(49), 18099-18111.
23. Yin H, Qi HJ, Fan F, Zhu T, Wang B, Wei Y (2015) Griffith criterion for brittle fracture in graphene. Nano letters, 15(3), 1918-1924.
24. Mishnaevsky G, Leon (2014) Graphene reinforced nanocomposites: 3D simulation of damage and fracture. Computational Materials Science, 95, 684-692.
25. Gf A, Fs B, Fs C, Dh A, Is D, Cf B, et al (2021) Finite element and experimental studies on the machining process of polymer/graphene nanoplatelet nanocomposites.
26. Su Y, Li Z, Yu Y, Zhao L, Li Z, Guo Q, et al (2017) Composite structural modeling and tensile mechanical behavior of graphene reinforced metal matrix composites. Science China Materials.

Supplementary Files

This is a list of supplementary files associated with this preprint. Click to download.

- video1.mp4
- video2.mp4